Heliyon

Received:
27 December 2018
Revised:
20 March 2019
Accepted:
27 March 2019

Cite as: Rajasekhar Chokkareddy, Gan G. Redhi, T. Karthick. A lignin polymer nanocomposite based electrochemical sensor for the sensitive detection of chlorogenic acid in coffee samples.
Heliyon 5 (2019) e01457.
doi: 10.1016/j.heliyon.2019.e01457

A lignin polymer nanocomposite based electrochemical sensor for the sensitive detection of chlorogenic acid in coffee samples

Rajasekhar Chokkareddy [a,**], **Gan G. Redhi** [a,*], **T. Karthick** [b]

[a] *Department of Chemistry, Durban University of Technology, Durban, 4000, South Africa*

[b] *Institute of Organic Chemistry and Biochemistry, Academy of Sciences, Flemingovo náměstí 2, 16610 Prague, Czech Republic*

[*] Corresponding author.

[**] Corresponding author.

E-mail addresses: chokkareddys@gmail.com (R. Chokkareddy), redhigg@dut.ac.za (G.G. Redhi).

Abstract

In this study, an innovative nanocomposite of multiwalled carbon nanotubes (MWCNTs), copper oxide nanoparticles (CuONPs) and lignin (LGN) polymer were successfully synthesized and used to modify the glassy carbon electrode for the determination of chlorogenic acid (CGA). Cyclic voltammetry (CV) emphasised a quasi-reversible, adsorption controlled and pH dependent electrode procedure. In cyclic voltammetry a pair of well distinct redox peaks of CGA were observed at the LGN-MWCNTs-CuONPs-GCE in 0.1 M phosphate buffer solution (PBS), at pH 2. The synthesized nanoparticles and nanocomposites were characterized by Fourier transformation infrared spectroscopy (FTIR), transmission electron microscopy (TEM) and x-ray diffraction (XRD) analyses. Differential pulse voltammetry (DPV) was applied to the anodic peak and used for the quantitative detection of CGA. Under optimal conditions, the proposed sensor showed linear responses from 5 μM to 50 μM, the linear regression

https://doi.org/10.1016/j.heliyon.2019.e01457

equation I_{pa} (μA) = 2.6074 C-5.1027 (R^2 = 0.995), whilst the limit of detection (LOD) and limit of quantifications (LOQ) were found to be 0.0125 μM and 0.2631 μM respectively. The LGN-MWCNTs-CuONPs-GCE were applied to detect the CGA in real coffee samples with the recovery ranging from 97 to 106 %. The developed sensor was successfully applied for the analysis of CGA content in the coffee samples. In addition, electrophilic, nucleophilic reactions and chlorogenic acid docking studies were carried out to better understand the redox mechanisms and were supported by density functional theory calculations.

Keywords: Electrochemistry, Analytical chemistry, Materials chemistry

1. Introduction

Chlorogenic acid (CGA) contains a large group of natural polyphenolic compounds. CGA is a family of various esters (mono-, di-, tri- and mixed esters) made from (-)-quinic acid and certain hydroxycinnamic acids, usually caffeic, ferulic and p-coumaric acids [1]. The chemical structure of CGA is shown in Fig. 1. These polyphenolic compounds are plant metabolites and broadly spread in many plant kingdoms as well as beverages and foods, especially in coffee that has one of the highest concentrations of CGA of all plant derived constituents [2, 3]. CGA is found substantially in various forms of coffee beans. It is also found in numerous fruit and vegetables of human diet, such as apple, pear, peach, plum, apricot, cherry, blueberry and strawberry [4]. Moreover, CGA are phenolic acids with vicinal hydroxyl groups on aromatic residues that are found to occur as a result of esterification of cinnamic acids, which include caffeic, ferulic, p-coumaric acids with quinic acid [5, 6].

Based on the ester substituent, chlorogenic acids are further classified into more subgroups such as: caffeoylquinic acids (CQAs), feruloylquinic acids (FQAs), p-coumaroylquinic acids (p-CoQAs), etc. Coffee is known to be the major source of dietary CGA intake of humans and coffee is prepared from the roasted seeds (beans)

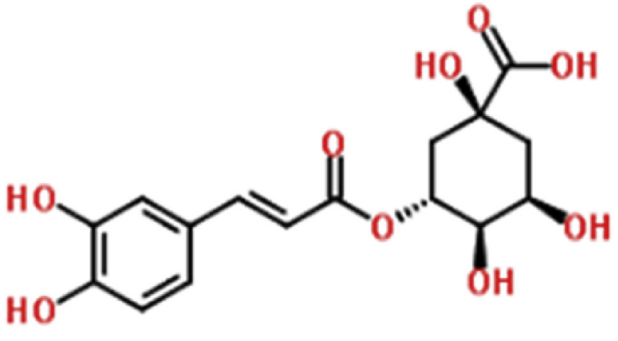

Fig. 1. Molecular structure of chlorogenic acid.

https://doi.org/10.1016/j.heliyon.2019.e01457

derived from a bush of the genus coffea, 66% of the world production is Coffea Arabica and 34% from Coffea canophora [7]. Traditionally, it has been believed that drinking large amount of coffee may cause liver diseases. In contrast, many reports have specified that a diet rich in CGA compounds plays an excessive role in inhibiting several diseases related with oxidative stress such as cardiovascular, cancer, aging and neurodegenerative diseases [8]. Moreover, in the last few decades the biological effects of coffee on human organisms have been widely investigated and current report suggests that drinking coffee in an appropriate amount, has a very good impact on the cardiovascular system and metabolism of carbohydrate and lipid functions [9]. CGA has been found to be active for the reduction of glucose levels in type 2 diabetes [10, 11]. Consequently, quantitative measurement of CGA in coffee samples have received a strong attention nowadays. Many methods have been developed so far for the detection of CGA in coffee beans and other plants viz., high performance liquid chromatography (HPLC) [12], capillary electrophoresis [13], micellar electrokinetic chromatography [14], near infrared spectroscopy [15] and electrochemical methods [3, 10, 16, 17, 18, 19, 20, 21, 22]. However, the traditional spectrophotometry techniques are easily inhibited by the other interfering samples present in the real coffee samples. In order to overcome the limitations, HPLC can be a superior choice for the determination of CGA, although the high cost columns and the high waste of samples severely control the enlargement of these methods. To the best of our knowledge, the electrochemical detection of CGA has been barely described in the literature. Moreover, in recent years electrochemical techniques have received much attention for the detection of CGA because of their important advantages i.e. rapid response, low cost, high efficiency and relatively simple analytical procedures. The electrochemical methods have been upgraded with the innovation of multiwalled carbon nanotubes (MWCNTs) as electrochemical sensors. MWCNTs are known for their unique geometrical, electronic and mechanical properties. In addition, polymer-modified electrodes (PMEs) offer good reproducibility and stability, increased active sites, strong adherence to the electrode surface and homogeneity in electrochemical deposition [23, 24, 25, 26, 27, 28, 29, 30]. To enhance the electrocatalytic activity for the CGA in the present work, copper oxide nanoparticles (CuONPs), lignin polymer (LGN) and glassy carbon electrode (GCE) were utilized. Furthermore, the electrochemical behaviour of CGA at LGN-MWCNTs-CuONPs-GCE was studied, and a sensitive electrochemical analysis technique of DPV was established for the detection of CGA. To explore certain properties of CGA such as HOMO-LUMO energy gaps, ionization potential, electron affinity, global hardness, electrophilicity index and the reactive sites for electrophilic and nucleophilic attack were investigated. Finally, the quantitative detection of CGA in real coffee samples was demonstrated using the newly developed electrochemical sensor.

https://doi.org/10.1016/j.heliyon.2019.e01457

2. Materials and methods

2.1. Chemicals and reagents

Chlorogenic acid (CGA), lignin polymer and multiwalled carbon nano tubes (outer diameter 7−15 nm and length 5 μm) were purchased from Sigma Aldrich (Durban, South Africa). Hydrochloric acid (HCl), disodium hydrogen orthophosphate (Na_2HPO_4), sodium dihydrogen orthophosphate (NaH_2PO_4), sodium hydroxide (NaOH), nitric acid (HNO_3), sulphuric acid (H_2SO_4), ethanol (C_2H_6O) copper sulphate ($CuSO_4$), acetic acid (CH_3COOH) and N, N dimethyl formamide (DMF) was obtained from Capital lab suppliers (Durban, South Africa). All the other reagents used were of analytical grade.

2.2. Instrumentation

The electrochemical measurements were performed using a 797 VA Computrace (Metrohm, Herisau, Switzerland) operated with a PC supplied by 797 VA Computrace and equipped with 1.3.1 software. A conventional three-electrode system with a GCE and fabricated electrode were used as the working electrode, whereas, Ag/AgCl (3 M KCl) reference electrode, and platinum wire were used as an auxiliary electrode. A Varian 800 Scimitar Fourier transform infrared spectroscopy (FT-IR) (SMM Instruments. Durban, South Africa) was used for the FT-IR characterization. A Transmission electron microscopy (TEM) JEM 2100 with a Lab 6 emitter (Max Oxford Instrument, JEOL Inc., Peabody, MA, USA) was engaged for the study of surface morphology of the nanoparticles and biosensor. X-ray diffraction study was carried out using a Bruker AXS D8 diffractometer with CuKα radiation ($\lambda = 1.5418$ E) at 40 kV over a 2θ range from 10° to 70° at a scanning rate of 0.05 min^{-1}. A Labcon 5019U ultra sonicator (Lasec, Durban, South Africa) was used for the ultrasonification of reagents. A Thermal Gravimetric Analysis (TGA) Differential Scanning Calorimetry (DSC) 1SF model 1346 (Columbus, OH, USA) with a $STAR^e$ software version 9.20 (Mettler Toledo) instrument was used for the thermal gravimetric analysis of the nanocomposite. In addition, the pH quantities were carried out on a CRISON micro pH 2000 digital pH meter using a combined electrode with an accuracy of ± 0.1 pH units.

2.3. Preparation of standard and supporting electrolyte

CGA solution (0.1 mM) was prepared quantitatively by evaluating an appropriate amount in a 10 mL volumetric flask and diluted with deionized water up to the calibration mark. Similarly, 0.1 M phosphate buffer solution was prepared from sodium dihydrogen orthophosphate and disodium hydrogen orthophosphate, and dissolved in a 250 mL volumetric flask. The optimum pH 2 was attained by quantitatively

https://doi.org/10.1016/j.heliyon.2019.e01457

adding H_2SO_4/NaOH, and thereafter that the solution were stored at 4 °C. All aqueous solutions were prepared by using the deionized water.

2.4. Synthesis of nanoparticles

The CuONPs were prepared according to the earlier report with slight modification [31, 32], 0.53 g of $CuSO_4$ was dissolved in 50 mL of deionized water to prepare 0.2 M $CuSO_4$. This solution primarily appeared as a green coloured solution, and to this 1 mL of acetic acid was added. In another vessel 8 g of NaOH was dissolved in 25 mL of deionized water to get 8 M NaOH. In a drop wise manner, NaOH was added to the contents of $CuSO_4$ with continuous stirring, and was subjected to heating at 90 ^oC. In an instant, a black coloured precipitate was obtained. The precipitate was then centrifuged at 1000 ppm for 10 min, repeatedly washed 4 to 5 times with deionized water and then dried at 80 ^oC for 2 hours. The fine powder of CuONPs obtained was used for the characterization.

2.5. Real sample preparation

Aqueous extracts of the coffee samples were prepared by following the procedure outlined elsewhere [23]. 50 g of coffee from each sample was grounded using a mortar and pestle to obtain a uniform texture. An accurately weighed 4 g of sieved coffee from each sample was then boiled in 200 mL of distilled water in the temperature range 80−90 °C for 30 min while vigorously stirring with magnetic stirrer. The water extracted caffeine was finally separated from the residue by decantation and was ready for the DPV analysis.

2.6. Preparation and fabrication of the LGN-MWCNTs-CuONPs-GCE

The bare GCE was initially polished with 0.3 and 0.05 μm alumina powder and then washed with deionized water followed by electrochemical cleaning by cycling at a potential range from -0.5 V to 1.0 V for 40 cycles in acidified water (nitric acid + water). This procedure facilitated the elimination of any physisorbed or chemisorbed materials from the electrode surface. Then, 25 mg of MWCNTs was dissolved in 50 mL of N-N, dimethyl formamide solution and then kept for ultrasonication for about 60 min at 30 °C, resulting in the formation of a black suspension which was used for the fabrication of GCE [33, 34]. Similarly, 10 mg of MWCNTs and 10 mg of CuONPs were dispersed into 30 mL of DMF monitored by ultrasonication for about 90 min, to form a steady black suspension of MWCNTs-CuONPs. The resulting electrode was immersed in PBS (pH 2) and it was activated potentiodynamically by scanning the potential between + 0.2 and +1 V for five cycles, at a scan rate of 100 mVs^{-1}. Thereafter, the activated electrode was fabricated

https://doi.org/10.1016/j.heliyon.2019.e01457

with 5 μL MWCNTs-CuONPs nanocomposite, and then dried in an oven at 50 °C for 5 min. After that the modified electrode was dipped in the LGN solution for 15 min at room temperature and the LGN modified electrode was rinsed with deionized water to remove physically adsorbed and unreacted species from the electrode surface. The resulting LGN modified electrode was then used for the detection of CGA.

3. Results and discussion

3.1. Electrochemical characterization of chlorogenic acid

The LGN-MWCNTs-CuONPs-GCE hybrid electrode was characterized by TEM, TGA, XRD and FTIR. Fig. 2A shows the FT-IR spectrum of the CuONPs in the range of 400−4000 cm^{-1}. The two characteristic bands observed at 509 cm^{-1} and 604 cm^{-1} can be assigned to the CuONPs [35]. For the range from 605-660 cm^{-1} no other IR active mode was observed in CuONPs. Moreover, the peak at 871 cm^{-1} was responsible for = C-H bending, 1122 cm^{-1} for C-O stretching, 1629 cm^{-1} for O-H stretching and 3396 cm^{-1} for O-H stretching vibrations, respectively [36]. The XRD pattern for the CuONPs is shown in (Fig. 2B). The XRD peaks confirmed that the formation of CuONPs from each precursor was in monoclinic phase, no other impurity peaks was observed in the XRD pattern. According to

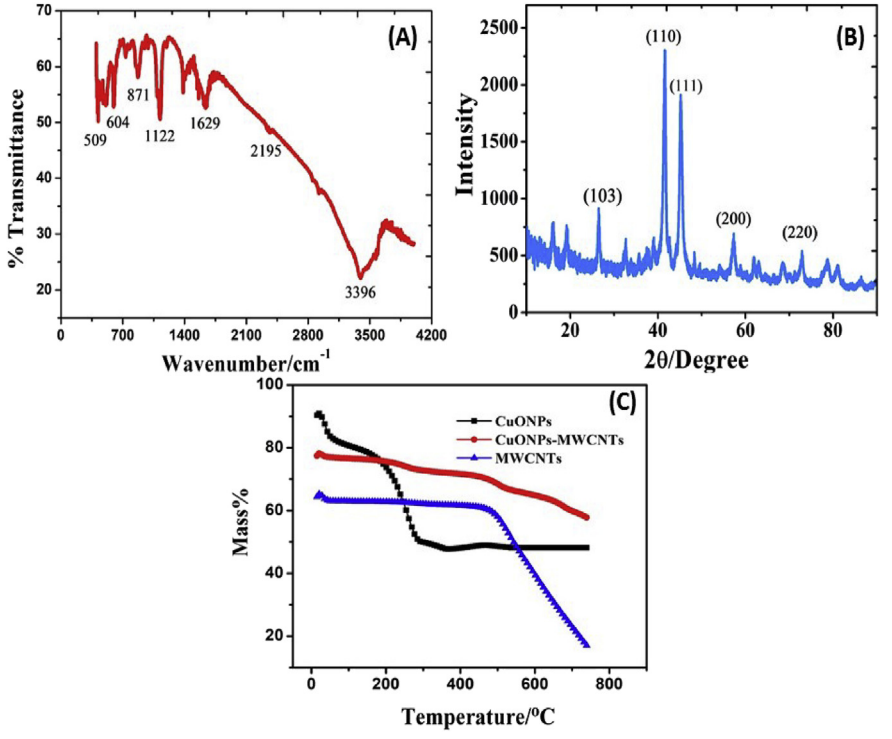

Fig. 2. (A) FTIR spectrum of CuONPs (B) XRD pattern of CuONPs (C) TGA curves for (i) MWCNTs (blue colour line), (ii) CuONPs (black colour line) and (iii) CuONPs-MWCNTs (red colour line).

https://doi.org/10.1016/j.heliyon.2019.e01457

previous literature the XRD pattern displays two main diffractions at 2θ = 36.6° (110) and 2θ = 38.8° (111) and these were ascribed to the formation of the CuONPs in face centered cubic (FCC) and monoclinic crystal lattices [37]. Fig. 2C shows the TGA curves for MWCNTs (blue colour line), CuONPs (black colour line) and CuONPs-MWCNTs (red colour line). MWCNTs exhibited a major decrement in mass around 570 °C. In the TGA curve of CuONPs, the loss of mass occurred twice; the minor one at 100 °C due to evaporation of water, the second one at above 400 °C may due to the removal of organic moieties. Finally, the CuONPs decorated on the MWCNTs show different TGA curves, and it loses minor mass at below 600 °C, due to the evaporation of some organic moieties. Fig. 3A displays a distinctive TEM image of the synthesized CuONPs. Furthermore, a combination of nanoscale particles is visibly observed and displaying an even distribution of particle size, with an average size of 10−25 nm. Fig. 3B shows the pure MWCNTS, these MWCNTs are hollow inner tube like structure. However, in Fig. 3C describes the MWCNTs network decorated with CuONPs and lignin polymer in a form of mixture sheets. In addition, the strong π−π non-covalent interactions that occur between the tubular structure of MWCNTs, CuONPs and lignin polymer is motivated by the

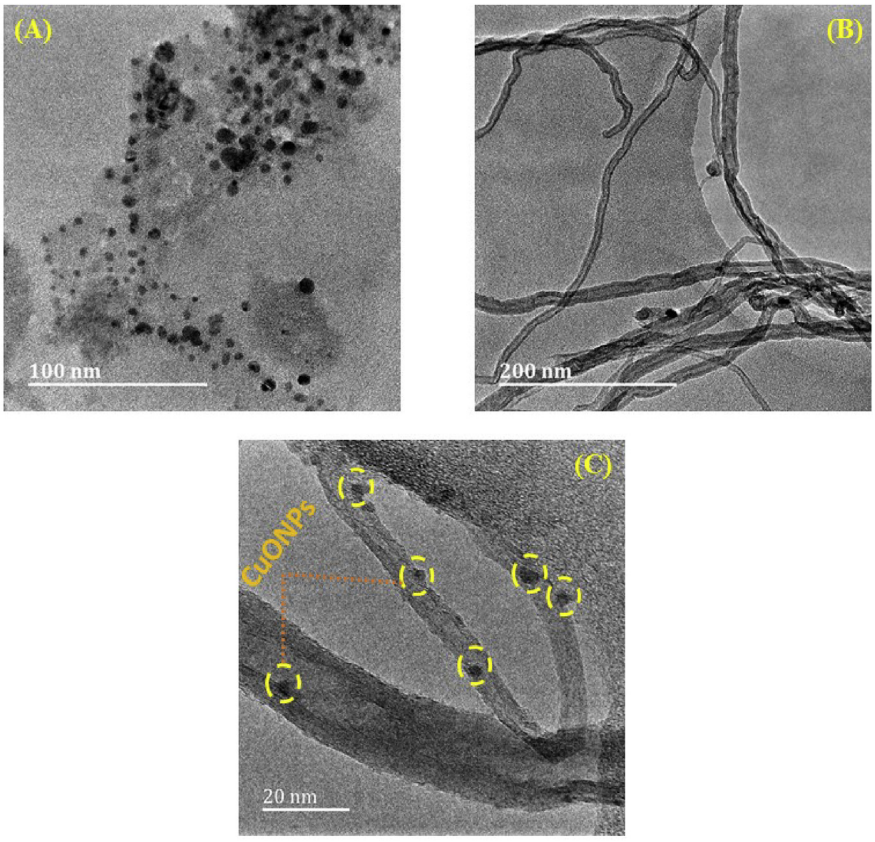

Fig. 3. TEM images for (A) pure CuONPs (B) pure MWCNTs and (C) CuONPs decorated on MWCNTs surface.

https://doi.org/10.1016/j.heliyon.2019.e01457

hydrophobic surface which plays a crucial role towards the formation of LGN-MWCNTs-CuONPs mixture.

3.2. Effect of pH and deposition time

The chlorogenic acid has o-hydroquionone moiety, and it was anticipated that the redox response of chlorogenic acid would be pH dependent. The redox reaction of 0.1 mM CGA was studied over the pH range of 2−9 in phosphate buffer solution by cyclic voltammetry which is displayed in Fig. 4A. In addition, from Fig. 4A the anodic and cathodic peak currents gradually increases with increasing the pH value from 2.0 to 5.0, whilst the peak currents decrease with increasing the pH value above 6.0, and the related anodic and cathodic peak potential was also shifted more towards the negative potential side with increase of the pH. Moreover, in acidic medium the o-hydroquione is converted into quinone, it is a single step two-electron and proton transfer, while in alkaline pH the electrochemical characterization does not involve the proton transfer and is only a case of two electron reduction. Hence the 0.1 M

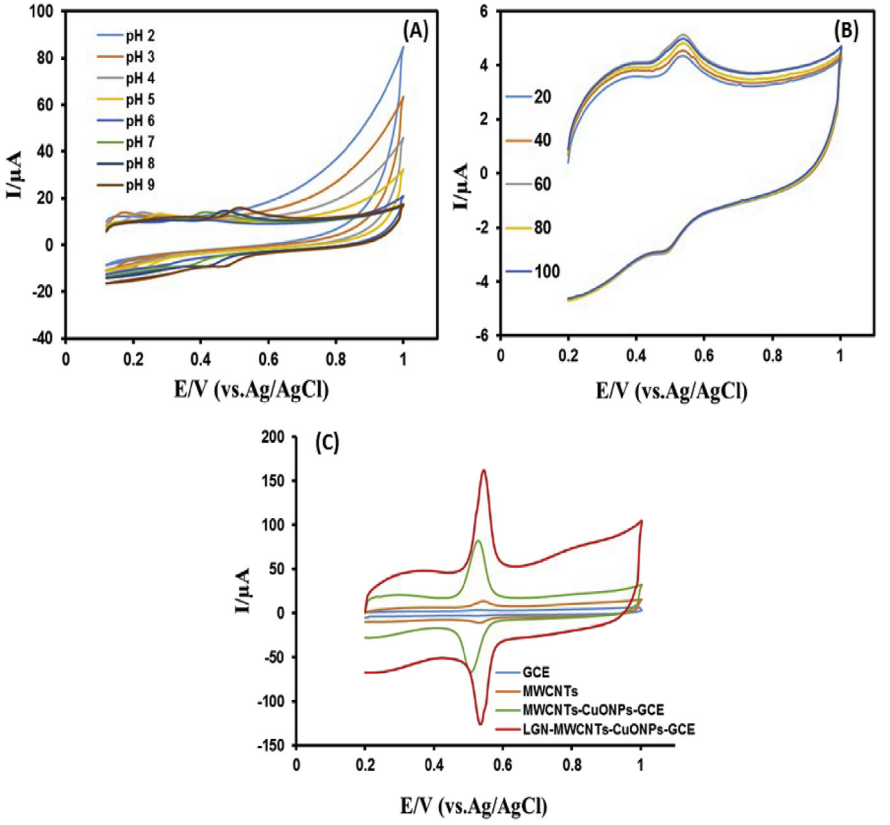

Fig. 4. (A) Cyclic voltammograms of 0.1mM CGA in different pH of PBS buffer solution at scan rate of 0.01 mVs^{-1}. Inset is the variation of anodic peak potential with buffer pH. (B) Various deposition times (20, 40, 60, 80, and 100) on peak current. (C) Cyclic Voltammograms of 0.1 mM CGA at bare (i) GCE, (ii) MWCNTs-GCE (iii) MWCNTs-CuONPs-GCE, and (iv) LGN- MWCNTs-CuONPs-GCE.

https://doi.org/10.1016/j.heliyon.2019.e01457

phosphate buffer solution with pH 2 is an excellent medium for electron-proton transfer between the solution and the electrode. Therefore 0.1 mM CGA with pH 2 was chosen as a supporting electrolyte for the entire determination. Fig. 4B displays the effect of deposition time from 20 s to 100 s. The currents of chlorogenic acid increased gradually from 20 s to 60 s, after that at 80 s and 100 s the peak current are decreased. This indicate that a lower deposition time initiated more CGA to deposit onto the modified electrode surface. Hence, 60 s was preferred as the optimal deposition time for entire studies.

3.3. Electrochemical characterization of LGN-MWCNTs-CuONPs modified electrode

The electrochemical behaviour of the bare GCE, MWCNTs-GCE, MWCNTs-CuONPs-GCE and LGN-MWCNTs-GCE were studied by using the cyclic voltammetry (Fig. 4C). For this investigation 0.1 M phosphate buffer solution was used as a supporting electrolyte. The scan rate is 0.01 mVs^{-1} with the potential range from 0.45 V to 0.55 V. The result displays that the bare GCE showed less electrochemical response; however, an observable pair of redox peaks were obtained. On comparing the electrode coating from Fig. 4C, the bare GCE has lesser sensitivity to CGA analyte. When coating an electrode with the MWCNTs, the sensitivity increases by five times when compared to sensitivity the bare electrode, with increasing current due to an electron transfer between the analyte and the electrode [38]. While coating the electrode with MWCNTs-CuONPs, the sensitivity of the electrode increases much higher with an increase in current. This is due to high surface reactivity and specific high surface area of the CuONPs at the electrode surface. Finally, the electrode was coated with nanocomposite and lignin polymer, the resulting voltammograms show an increase in peak current as well, which is brought about by the lignin where by it increases the active sites of the electrode [23] for homogeneous electrochemical deposition of CGA. The peak current increases while coating the electrode with the analyte in the order; MWCNTs < MWCNTs-CuONPs < LGN-MWCNTs-CuONPs, respectively. Moreover, the modified electrodes show good correlation with the increase in peak current height as displayed in Table 1.

Table 1. Different modified electrode correlations.

Coating	I_{pa}	I_{pc}
MWCNTs-GCE	I_{pa} (μA) = 763.53υ (mVs^{-1}) +11.004 R^2 = 0.9885	I_{pc} (μA) = -609.52υ (mVs^{-1}) +7.908 R^2 = 0.9888
MWCNTs-CuONPs-GCE	I_{pa} (μA) = -1059.42υ (mVs^{-1}) +14.392 R^2 = 0.9704	I_{pc} (μA) = -768.46υ (mVs^{-1}) +17.252 R^2 = 0.9441
LGN-MWCNTs-CuONPs-GCE	I_{pa} (μA) = 2356.9υ (mVs^{-1}) +35.233 R^2 = 0.9860	I_{pc} (μA) = 2124υ (mVs^{-1}) +35.233 R^2 = 0.9881

https://doi.org/10.1016/j.heliyon.2019.e01457

3.4. Effect of scan rate

The effect of the potential scan rate (υ) on electrochemical properties of the LGN-MWCNTs-CuONPs-GCE was also examined by cyclic voltammetry. The cyclic voltammograms were recorded for 0.1 mM of chlorogenic acid in 0.1 M phosphate buffer solution (pH 2) as a supporting electrolyte. Fig. 5A shows the scan rate ranges from 0.01 to 0.1 mVs^{-1}. As revealed in Fig. 5B, when the scan rate was different from 0.01 to 0.1 mVs^{-1} in 0.1 mM solution of CGA, a linear dependence of the redox response upon the scan rate (υ) was detected, and it indicates an adsorption controlled process. Fig. 5C shown is the plot of logarithm of peak current against scan rate. The plot gives straight lines with slopes of 0.821 and 0.810 for anodic and cathodic currents, respectively. These values are very close to the theoretical value estimated for an ideal diffusion controlled electrochemical reaction [10]. Adsorption controlled electrochemical reaction process is quasi-reversible, the effect of the scan rate on both the oxidation and reduction, the oxidation peak shifted

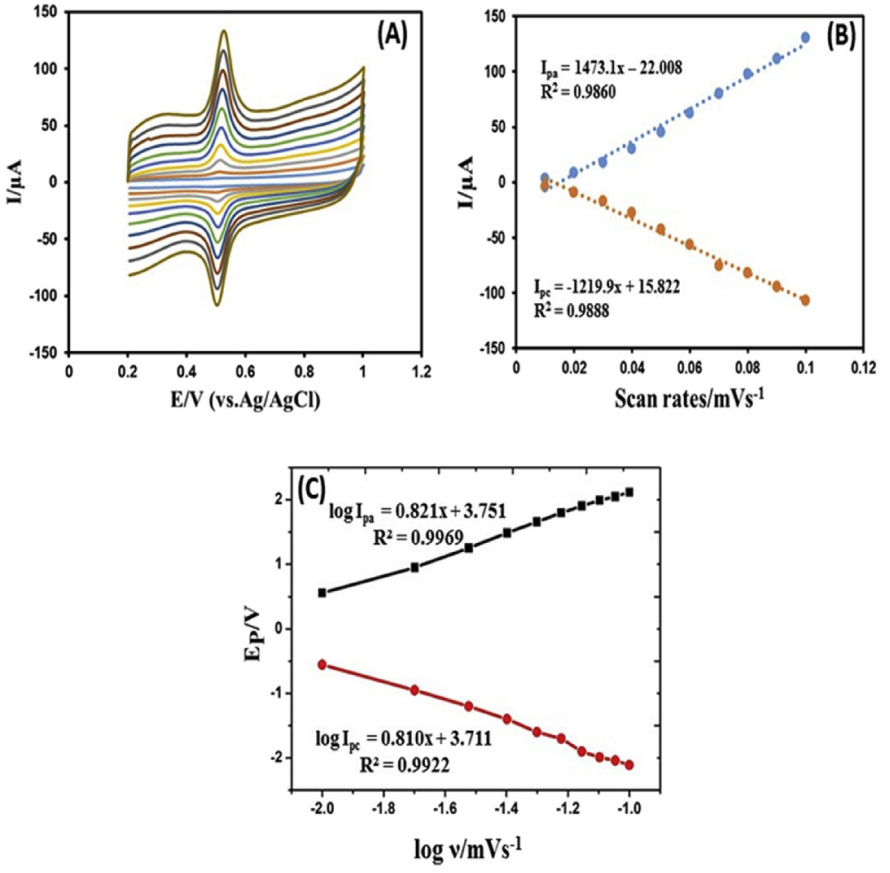

Fig. 5. (A) Cyclic voltammetry responses of the fabricated electrode in PBS buffer solution (pH 2) at scan rates (inner to outer) 0.01, 0.02, 0.03, 0.04, 0.05, 0.06, 0.07, 0.08, 0.09, and 0.1 mVs^{-1}. (B) The plot of anodic and cathodic peak current vs. scan rate (C) Variation of peak potentials vs. logarithm of scan rate.

https://doi.org/10.1016/j.heliyon.2019.e01457

slightly positive whilst the reduction peak moved slightly negative side as the scan rate increases. Both the oxidation peak current (I_{pa}) and reduction peak current (I_{Pc}) increase linearly with the scan rate (υ), particularly within the scan range from 0.01 to 0.1 mVs^{-1}, where the linear regression equation are expressed as I_{pa} (μA) = 2356.9υ (mVs^{-1}) + 35.233 (R^2 = 0.9860) and I_{pc} (μA) = 2124υ (mVs^{-1}) + 35.233 (R^2 = 0.9881). This effect may be due to the increasing of the electro-active site on the glassy carbon electrode. During the reaction process, peak-to-peak separation (ΔE_p) was slightly increased. By using the formal potential Eq. (1),

$$\Delta E_p = \frac{0.059}{n} V \tag{1}$$

where ΔE is the difference in peak potential, *n* number of electrons transferred between the electrolyte and the electrode, and *n* which was calculated to be 2.4. The redox reaction of chlorogenic acid is based on the transfer of two-electrons and two protons. In addition, the proposed mechanism of electro-oxidation for the chlorogenic acid is proceeded by two steps; (i) pre-dissociation of a proton to form the mono anionic species (ii) the mono anionic species is then oxidized to give a radical. The resulting radical undergoes rapidly a second electronic transfer to form a carbocation, which is rapidly dehydrated to yield the corresponding quinone, which is then reduced into chlorogenic acid during the reverse scan. The schematic illustration of the redox reaction mechanism is displayed in Fig. 6.

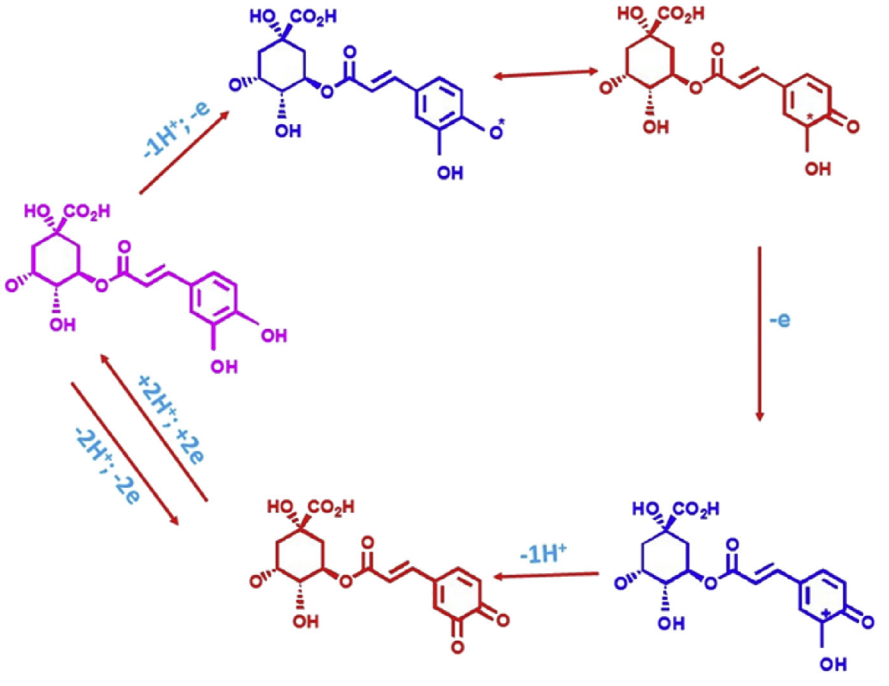

Fig. 6. Schematic illustration of the redox reaction mechanism of chlorogenic acid.

https://doi.org/10.1016/j.heliyon.2019.e01457

3.5. Determination of chlorogenic acid

Since it is a dynamic voltammetric technique with well-known advantages, containing good discrimination against background current and limit of detection, differential pulse voltammetry (DPV) was used for the quantification of chlorogenic acid content of coffee samples refined in different coffee samples in South Africa. DPV was utilized under the optimized conditions (accumulation time: 60 s, deposition potential: -0.124 V, equilibration time: 5.00 s) in order to maximize sensitivity for the quantification of chlorogenic acid. Moreover, the linear regression curve (peak current *versus* CGA concentration) in the range of 5−55 μM with the $R^2 = 0.9950$ was obtained (Fig. 7). In addition, the sensitivity of the proposed technique was tested in terms of the limit of detection (LOD) and limits of quantification (LOQ) values. The LOD and LOQ were calculated using the following equations:

$$\mathrm{LOD} = \frac{3S}{m} \tag{2}$$

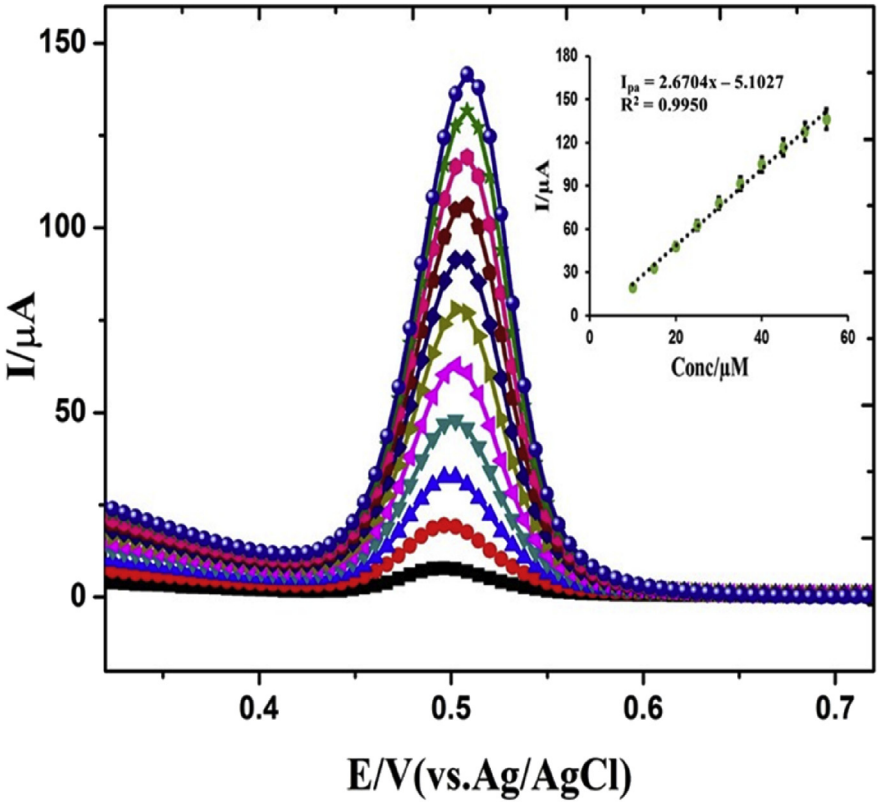

Fig. 7. Differential pulse voltammograms for different concentrations of chlorogenic acid in the range from 5 μM to 50 μM and insert corresponding linear calibration curve of peak current vs. CGA concentration.

https://doi.org/10.1016/j.heliyon.2019.e01457

$$LOQ = \frac{10S}{m} \quad (3)$$

where s is the standard deviation, and m is the slope of calibration plot. The LOD and LOQ were found to be 0.0125 μM and 0.2631 μM, respectively. The values obtained in this work are well matched with the earlier reports [20, 39, 40, 41] and are presented in Table 2.

3.6. Real samples analysis

The reliabilty and applicability of the LGN-MWCNTs-CuONPs modified sensor was estimated by the detection of chlorogenic acid in real coffee samples by a standard-addition procedure. Prior to the examination, the coffee samples were ground into fine powder with mortar and pestle, then accurately weighed. In addition, to prepare the 0.1 mM coffee sample solution, the coffee residue was transferred into a 10 mL volummetric flask, then dissolved and brought to volume by 0.1 M PBS (pH 2). The sample investigation was carried out by DPV method using a recovery test process and the results are summarized in Table 3. The recovery of the real samples ranging from 97 to 106%, and the RSD values were less than 4%. The obtained results proved that the proposed sensor can be used effectively for the detection of chlorogenic acid in real coffee samples.

3.7. Electrophilic and nucleophilic sites of chlorogenic acid global reactivity descriptors

To explore the sites which are favorable to electrophilic and nucleophilic reactions, quantum chemical calculations were performed with density functional theory (DFT) and standard basis set 6-311++G(d,p). For the precise analysis of active sites, both the electrostatic potential (ESP) charges and hirshfeld charges were computed. The electrostatic potential map generated on the basis of electron density

Table 2. Comparison of our research with various electroanalytical techniques for chlorogenic acid detection.

Electrode	Technique	Detection limit	Buffer & pH	Ref
Poly (aminosulfonic acid) modified glassy carbon electrode	CV	8.0×10^{-8} μM	Phosphate buffer solution (8)	[20]
Multi-walled carbon nanotubes modified screen-printed electrode	DPV	0.12 μg/mL	Acetic acid-sodium acetate buffer solution (6.2)	[39]
Boron-doped diamond electrode	SWV	0.049 μg mL^{-1}	Britton−Robinson buffer (3.0)	[40]
Carbon nanotubes modified screen-printed electrode	CV&DPV	3.25 μM	Acetic acid-sodium acetate buffer solution (6.2)	[41]
Multi-walled carbon nanotubes, copper oxide nanoparticles and lignin polymer modified glassy carbon electrode	CV&DPV	0.0125 μM	Phosphate buffer solution (2)	This Work

https://doi.org/10.1016/j.heliyon.2019.e01457

Table 3. Chlorogenic acid recovery information in the samples of coffee extracts based on the presented sensor.

Coffee Robusta			Coffee Nescafe		
Added (μM)	**Found (μM)**	**Recovery (%) ±RSD (%)**	**Added (μM)**	**Found (μM)**	**Recovery (%) ± RSD (%)**
5.00	5 ± 0.15	97%	5.00	5 ± 0.13	97%
10.00	10 ± 0.2	99%	10.00	9 ± 0.4	106%
15.00	14 ± 0.9	106%	15.00	15 ± 0.2	99%
20.00	20 ± 0.13	99%	20.00	20 ± 0.18	99%

indicates the sites susceptible for electrophilic and nucleophilic reactions. Since the oxygen atom is more electronegative than hydrogen, the hydroxyl groups behave as a nucleophile. The blue colour surface over the aromatic hydrogen atoms reflect their electrophilic nature as shown in Fig. 8. For more precise analyis of electrophilic and nucleophilic sites, Fukui functions were analysed by incorporating hirshfeld charges (q_A) in the following expressions [32].

$$f_A^0(\overrightarrow{r}) = \frac{1}{2}\left[q_{A(N-1)} - q_{A(N+1)}\right] \; \textit{for neutral radical}$$

$$f_A^+(\overrightarrow{r}) = \frac{1}{2}\left[q_{A(N)} - q_{A(N+1)}\right] \; \textit{for nucleophilic attack}$$

$$f_A^-(\overrightarrow{r}) = \frac{1}{2}\left[q_{A(N-1)} - q_{A(N)}\right] \; \textit{for electrophilic attack}$$

where $f_A^0(\overrightarrow{r}), f_A^+(\overrightarrow{r})\ and\ f_A^-(\overrightarrow{r})$ are the Fukui functions corresponding to neutral radical, nucleophilic attack and electrophilic attack, respectively. Table 4 presents the predicted electrostatic point charges, hirshfeld charges and fukui functions of individual atoms of chlorogenic acid. The relative electrophilicity

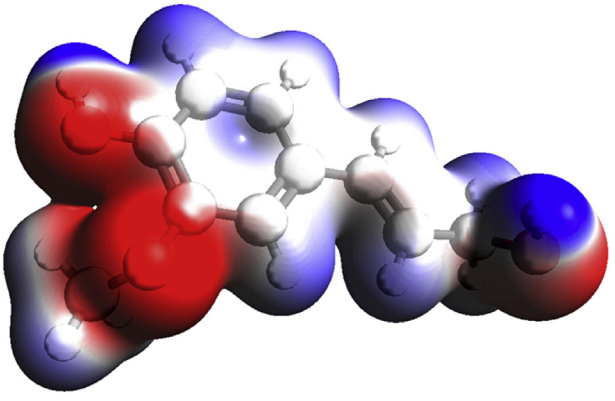

Fig. 8. Electrostatic potential surface of chlorogenic acid indicates electrophilic (blue) and nucleophilic sites (red).

https://doi.org/10.1016/j.heliyon.2019.e01457

Table 4. Charges (Electrostatic, hirshfeld) and Fukui functions of chlorogenic acid.

Atom	Charge				Fukui Functions[a]			$\frac{f_A^+(\vec{r})}{f_A^-(\vec{r})}$	$\frac{f_A^-(\vec{r})}{f_A^+(\vec{r})}$
	Electrostatic	hirshfeld							
		$q_{A(N)}$	$q_{A(N-1)}$	$q_{A(N+1)}$	$f_A^0(\vec{r})$	$f_A^+(\vec{r})$	$f_A^-(\vec{r})$		
O1	−0.3656	−0.1569	−0.1677	−0.1284	1.0774	2.8514	1.9644	0.3778	2.6466
O2	−0.0067	−0.0140	−0.2390	0.1142	22.4919	12.8256	17.65875	1.7537	0.5702
O3	−0.1874	−0.0929	−0.1988	−0.0187	10.5953	7.4199	9.0076	1.4280	0.7003
C4	0.2342	−0.0163	−0.0420	0.0481	2.5712	6.4463	4.50875	0.3989	2.5071
C5	−0.0731	0.0046	−0.0567	0.0613	6.1278	5.6725	5.90015	1.0803	0.9257
C6	0.3044	0.0576	0.0365	0.1050	2.1073	4.7418	3.42455	0.4444	2.2502
C7	0.0546	−0.0020	−0.0528	0.0929	5.0782	9.4947	7.28645	0.5348	1.8697
C8	0.3849	0.0617	0.0148	0.1375	4.6882	7.5832	6.1357	0.6182	1.6175
C9	−0.0756	−0.0267	−0.1815	0.0591	15.4811	8.5794	12.03025	1.8045	0.5542
C10	0.0054	−0.0100	−0.0747	0.0713	6.4692	8.1325	7.30085	0.7955	1.2571
C11	0.0167	−0.0107	−0.0908	0.1166	8.0122	12.7305	10.37135	0.6294	1.5889
C12	0.4362	0.0928	0.0150	0.1676	7.7865	7.4796	7.63305	1.0410	0.9606
C13	0.2722	0.1129	0.0377	0.1733	7.515	6.0425	6.77875	1.2437	0.8041

[a] The presented Fukui functions are multiplied by 100.

$(f_A^+(\vec{r})/f_A^-(\vec{r}))$ and nucleophilicity $(f_A^-(\vec{r})/f_A^+(\vec{r}))$ indices that the oxygen atoms O2 and O3 are prone to be attacked by electrophiles and oxygen atom O1 in the methoxy group is susceptible to nucleophilic attack. Moreover, the energy gap between the HOMO and LUMO orbitals that enables an electron transition between the ground and excited states was calculated and is found to be 4.6913 eV. The electron transition belongs to HOMO and LUMO orbitals is estimated to be occurred at 255 nm and is attributed to $\pi \rightarrow \pi^*$. The orbital lobes shown in Fig. 9 displays the complementary nature of π-orbital overlapping over the benzene ring of HOMO and LUMO surfaces. Based on the energy of HOMO and LUMO

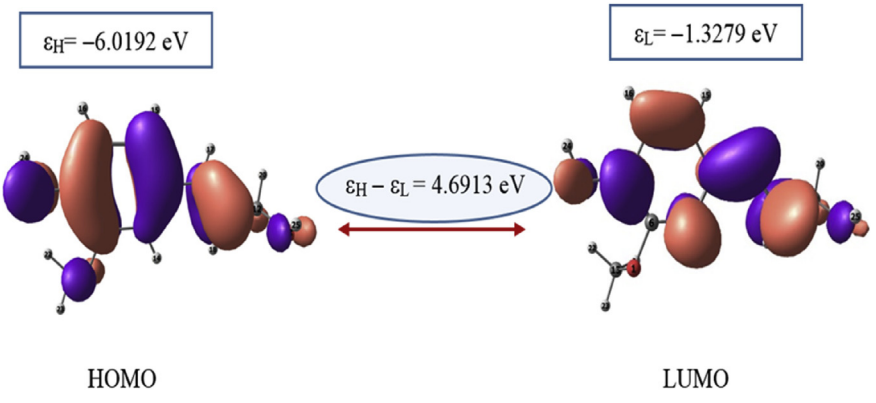

Fig. 9. Orbital lobes on the HOMO and LUMO surfaces.

https://doi.org/10.1016/j.heliyon.2019.e01457

Table 5. Local reactivity descriptors (in eV) of chlorogenic acid.

Energy of HOMO (ε_H) (ev)	Energy of LUMO (ε_L) (ev)	Energy gap ($\varepsilon_H - \varepsilon_L$) (ev)	Electronegativity (χ)	Chemical potential (μ)	Global hardness (η)	Global softness (S)	Global electrophilicity index (W)
−6.0192	−1.3279	4.6913	3.6736	−3.6736	2.3457	0.2132	2.8766

orbitals, certain local reactivity descriptors useful to understand the reactivity of chlorogenic acid is proposed (Table 5).

3.8. Interfernce studies

The established technique must be sensitive and selective to the analyte for real sample applications. Hence, other potential electroactive species should not have a substantial interference effect on the analytical signal. The interferences resulting from foreign substances on the redox reaction peak current of CGA at the surface of LGN-MWCNTs-CuONPs sensor under the optimal conditions was also calculated by DPV technique. For these investigations, the interfering species were added at various concentrations (a hundred fold) higher than the concentration of CGA (0.1 mM). The addition of filler materials (glucose, maltose, sucrose, and lactose), decomposing agent (starch), and organic substences produced no significant effect on the DPV response for CGA. The influence of certain cations (Cu^{2+}, Al^{3+}, Mg^{2+}, K^{+}, Fe^{3+}) and anions (Cl^{-}, CO_3^{2-}, NO_3^{-}) were calculated, and the results indicates that the ions were not influenced on the detection of CGA. The results are displayed in Table 6 and the tolerance limit was well-defined as the concentration which give an error of less than 5.0% in the detection of CGA.

3.9. Reproducibility and stability

The reproducibility of the proposed LGN-MWCNTs-CuONPs were determined. To study the reproducibility of the established method under the same conditions, four modified electrochemical sensors were independently examined in a 0.1 mM CGA solution. The result shows a promising RSD value of 1.78% (n = 6) which indicates

Table 6. The influence of some interfering substances on the detection of 0.1 mM of chlorogenic acid.

Interfering substances	Tolerance ratio/%
Glucose, maltose, sucorse and lactose	200
Cu^{2+}, Al^{3+}, Mg^{2+}, K^{+}, Fe^{3+}	300
Cl^{-}, CO_3^{2-}	70
NO_3^{-}	550
Uric acid, ascorbic acid	300

https://doi.org/10.1016/j.heliyon.2019.e01457

that the results were reproducible using LGN-MWCNTs-CuONPs. In addition, the stability of the LGN-MWCNTs-CuONPs sensor was examined by measuring its response current to 0.1 mM CGA when the modified electrode was stored in PBS (pH 2) at 4 °C for six weeks. It exhibited the response current and retained 93.2% of its initial value after six weeks storage. The repeatability of the current response of LGN-MWCNTs-CuONPs electrode to 0.1 mM was estimated. The RSD is 4.1% for six succeeding determinations, indicating a good stability of the proposed electrochemical sensor.

4. Conclusions

A facile electrochemical sensor based on LGN-MWCNTs-CuONPs nanocomposite was effectively fabricated. The electrode shows significant response for the electro-redox reactions of CGA on the surface of the LGN-MWCNTs-CuONPs-GCE associated to unmodified GCE as well as changes their redox potentials to the fewer ones. Under the optimized conditions the linear calibration diferential pulse voltammetry plots for the dtermination of CGA ranges from 5 to 55 μM and the limit of detection and limit of quantification found to be 0.0125 μM and 0.2631 μM, respectively. In addition, this study establishes the useful analytical efficiency of the prepared fabricated electrode for the determination of cholorogenic acid in real coffee samples. The applicability of the sensor was tested with real coffee samples, and the good performance of the LGN-MWCNTs-CuONPs-GCE provided a promising alternative sensing application of CGA in the food industry. The proposed electrochimcal sensor signifies a good and easy technique for monitoring CGA in real samples demonstrating a excellent analytical performance due to its extended linear dynamic range, reproducibility and repeatability associated with a simplicity and low cost design.

Declarations

Author contribution statement

Gan G Redhi: Conceived and designed the experiments; Analyzed and interpreted the data; Wrote the paper.

Rajasekhar Chokkareddy: Conceived and designed the experiments; Performed the experiments; Analyzed and interpreted the data; Wrote the paper.

T. Karthick: Contributed reagents, materials, analysis tools or data.

Funding statement

This work was supported by Durban University of Technology.

https://doi.org/10.1016/j.heliyon.2019.e01457

Competing interest statement

The authors declare no conflict of interest.

Additional information

No additional information is available for this paper.

References

[1] M. Leopoldini, N. Russo, M. Toscano, The molecular basis of working mechanism of natural polyphenolic antioxidants, Food Chem. 125 (2011) 288−306.

[2] H. Xu, Q. Zheng, P. Yang, J. Liu, S. Xing, L. Jin, Electrochemical synthesis of silver nanoparticles-coated gold nanoporous film electrode and its application to amperometric detection for trace Cr(VI), Sci. China Chem. 54 (2011) 1004−1010.

[3] Y. Yardım, E. Keskin, Z. Şentürk, Voltammetric determination of mixtures of caffeine and chlorogenic acid in beverage samples using a boron-doped diamond electrode, Talanta 116 (2013) 1010−1017.

[4] X. Ma, M. Chen, Y. Wu, X. Li, S. Zhang, Studies on the electrochemical behavior of chlorogenic acid and its interaction with DNA at a graphene modified electrode, Int. J. Electrochem. Sci. 11 (2016) 8499−8511.

[5] N. Liang, D.D. Kitts, Role of chlorogenic acids in controlling oxidative and inflammatory stress conditions, Nutrients 8 (2015) 16.

[6] I. Tomac, M. Šeruga, E. Beinrohr, Characterization of chlorogenic acids in coffee by flow-through chronopotentiometry, Food Anal. Methods (2017) 1−10.

[7] A. Ayelign, K. Sabally, Determination of chlorogenic acids (CGA) in coffee beans using HPLC, Am. J. Res. Commun. 1 (2013) 78−91.

[8] L. Alvarez-Jubete, H. Wijngaard, E. Arendt, E. Gallagher, Polyphenol composition and in vitro antioxidant activity of amaranth, quinoa buckwheat and wheat as affected by sprouting and baking, Food Chem. 119 (2010) 770−778.

[9] S. Meng, J. Cao, Q. Feng, J. Peng, Y. Hu, Roles of chlorogenic acid on regulating glucose and lipids metabolism: a review, Evid. Based Complement Altern. Med. 2013 (2013).

[10] N. Mohammadi, M. Najafi, N.B. Adeh, Highly defective mesoporous carbon − ionic liquid paste electrode as sensitive voltammetric sensor for determination of chlorogenic acid in herbal extracts, Sensor. Actuator. B Chem. 243 (2017) 838−846.

https://doi.org/10.1016/j.heliyon.2019.e01457

[11] B.K. Bassoli, P. Cassolla, G.R. Borba-Murad, J. Constantin, C.L. Salgueiro-Pagadigorria, R.B. Bazotte, et al., Chlorogenic acid reduces the plasma glucose peak in the oral glucose tolerance test: effects on hepatic glucose release and glycaemia, Cell Biochem. Funct. Cell. Biochem. Modulat. Act. Agents Dis. 26 (2008) 320–328.

[12] G.M. Weisz, L. Schneider, U. Schweiggert, D.R. Kammerer, R. Carle, Sustainable sunflower processing-I. Development of a process for the adsorptive decolorization of sunflower [Helianthus annuus L] protein extracts, Innov. Food Sci. Emerg. Technol. 11 (2010) 733–741.

[13] E. Hurtado-Fernandez, M. Gomez-Romero, A. Carrasco-Pancorbo, A. Fernández-Gutiérrez, Application and potential of capillary electroseparation methods to determine antioxidant phenolic compounds from plant food material, J. Pharm. Biomed. Anal. 53 (2010) 1130–1160.

[14] Z. Es'haghi, M.A. Golsefidi, A. Saify, A.A. Tanha, Z. Rezaeifar, Z. Alian-Nezhadi, Carbon nanotube reinforced hollow fiber solid/liquid phase microextraction: a novel extraction technique for the measurement of caffeic acid in Echinacea purpurea herbal extracts combined with high-performance liquid chromatography, J. Chromatogr. A 1217 (2010) 2768–2775.

[15] Y. FU, Determination of the contents of chlorogenic acid and phillyrin of shuanghuanglian oral fluid using NIRS, Spectrosc. Spectr. Anal. 30 (2010) 358–362.

[16] M.L. de Carvalho, M. Santhiago, R.A. Peralta, A. Neves, G.A. Micke, I.C. Vieira, Determination of chlorogenic acid in coffee using a biomimetic sensor based on a new tetranuclear copper (II) complex, Talanta 77 (2008) 394–399.

[17] S.C. Fernandes, S.K. Moccelini, C.W. Scheeren, P. Migowski, J. Dupont, M. Heller, et al., Biosensor for chlorogenic acid based on an ionic liquid containing iridium nanoparticles and polyphenol oxidase, Talanta 79 (2009) 222–228.

[18] N. Alpar, Y. Yardım, Z. Şentürk, Selective and simultaneous determination of total chlorogenic acids, vanillin and caffeine in foods and beverages by adsorptive stripping voltammetry using a cathodically pretreated boron-doped diamond electrode, Sensor. Actuator. B Chem. 257 (2018) 398–408.

[19] C.M. Ribeiro, E.M. Miguel, J.d.S. Silva, C.B. da Silva, M.O. Goulart, L.T. Kubota, et al., Application of a nanostructured platform and imprinted sol-gel film for determination of chlorogenic acid in food samples, Talanta 156 (2016) 119–125.

https://doi.org/10.1016/j.heliyon.2019.e01457

[20] X. Ma, H. Yang, H. Xiong, X. Li, J. Gao, Y. Gao, Electrochemical behavior and determination of chlorogenic acid based on multi-walled carbon nanotubes modified screen-printed electrode, Sensors 16 (2016) 1797.

[21] I. Vasilescu, S.A. Eremia, R. Penu, C. Albu, A. Radoi, S.C. Litescu, et al., Disposable dual sensor array for simultaneous determination of chlorogenic acid and caffeine from coffee, RSC Adv. 5 (2015) 261−268.

[22] M. Chao, X. Ma, Voltammetric determination of chlorogenic acid in pharmaceutical products using poly (aminosulfonic acid) modified glassy carbon electrode, J. Food Drug Anal. 22 (2014) 512−519.

[23] M. Amare, S. Aklog, Electrochemical determination of caffeine content in Ethiopian coffee samples using lignin modified glassy carbon electrode, J. Anal. Methods Chem. 2017 (2017).

[24] C.E. Zou, B. Yang, D. Bin, J. Wang, S. Li, P. Yang, et al., Electrochemical synthesis of gold nanoparticles decorated flower-like graphene for high sensitivity detection of nitrite, J. Colloid Interface Sci. 488 (2017) 135−141.

[25] S. Li, B. Yang, C. Wang, J. Wang, Y. Feng, B. Yan, et al., A facile and green fabrication of Cu_2O-Au/NG nanocomposites for sensitive electrochemical determination of rutin, J. Electroanal. Chem. 786 (2017) 20−27.

[26] H. Beitollahi, S. Nekooei, M. Torkzadeh-Mahani, Amperometric immunosensor for prolactin hormone measurement using antibodies loaded on a nano-Au monolayer modified ionic liquid carbon paste electrode, Talanta 188 (2018) 701−707.

[27] H. Beitollahi, H. Karimi-Maleh, H. Khabazzadeh, Nanomolar and selective determination of epinephrine in the presence of norepinephrine using carbon paste electrode modified with carbon nanotubes and novel 2-(4-oxo-3-phenyl-3, 4-dihydro-quinazolinyl)-N′-phenyl-hydrazinecarbothioamide, Anal. Chem. 80 (2008) 9848−9851.

[28] H. Beitollahi, S.G. Ivari, M. Torkzadeh-Mahani, Application of antibody−nanogold−ionic liquid−carbon paste electrode for sensitive electrochemical immunoassay of thyroid-stimulating hormone, Biosens. Bioelectron. 110 (2018) 97−102.

[29] H. Beitollahi, F. Garkani Nejad, Graphene oxide/ZnO nano composite for sensitive and selective electrochemical sensing of levodopa and tyrosine using modified graphite screen printed electrode, Electroanalysis 28 (2016) 2237−2244.

[30] H. Beitollahi, S. Nekooei, Application of a modified CuO nanoparticles carbon paste electrode for simultaneous determination of isoperenaline, acetaminophen and N-acetyl-L-cysteine, Electroanalysis 28 (2016) 645−653.

 https://doi.org/10.1016/j.heliyon.2019.e01457

[31] Y. Aparna, K.V. Rao, P.S. Subbarao, Preparation and characterization of CuO Nanoparticles by novel sol-gel technique, J. Nano Electron. Phys. 4 (2012), 3005-1, http://essuir.sumdu.edu.ua/handle/123456789/29602.

[32] R. Chokkareddy, N. Bhajanthri, G.G. Redhi, D.G. Redhi, Ultra-sensitive electrochemical sensor for the determination of pyrazinamide, Curr. Anal. Chem. 14 (2018) 391−398.

[33] R. Chokkareddy, N.K. Bhajanthri, G.G. Redhi, A novel electrode architecture for monitoring Rifampicin in various pharmaceuticals, Int. J. Electrochem. Sci. 12 (2017) 9190−9203.

[34] R. Chokkareddy, N.K. Bhajanthri, G.G. Redhi, An enzyme-induced novel biosensor for the sensitive electrochemical determination of isoniazid, Biosensors 7 (2017) 21.

[35] Z.N. Kayani, M. Umer, S. Riaz, S. Naseem, Characterization of copper oxide nanoparticles fabricated by the sol−gel method, J. Electron. Mater. 44 (2015) 3704−3709.

[36] D. Dodoo-Arhin, M. Leoni, P. Scardi, Microemulsion synthesis of copper oxide nanorod- like structures, Mol. Cryst. Liq. Cryst. 555 (2012) 17−31.

[37] J. Morales, L. Sanchez, F. Martin, J.R. Ramos-Barrado, M. Sánchez, Nanostructured CuO thin film electrodes prepared by spray pyrolysis: a simple method for enhancing the electrochemical performance of CuO in lithium cells, Electrochim. Acta 49 (2004) 4589−4597.

[38] W. Li, Y. Zheng, X. Fu, J. Peng, L. Ren, P. Wang, et al., Electrochemical characterization of multi-walled carbon nanotubes/polyvinyl alcohol coated electrodes for biological applications, Int. J. Electrochem. Sci. 8 (2013) 5738−5754.

[39] R.G. Parr, W. Yang, Density-Functional Theory of Atoms and Molecules, Vol. 16 of International Series of Monographs on Chemistry, Oxford University Press, New York, 1989.

[40] Y. Yardım, Electrochemical behavior of chlorogenic acid at a boron-doped diamond electrode and estimation of the antioxidant capacity in the coffee samples based on its oxidation peak, J. Food Sci. 77 (2012) C408−C413.

[41] X.-Y. Ma, H.-Q. Yang, H.-B. Xiong, X.-F. Li, J.-T. Gao, Y.-T. Gao, Electrochemical Behavior and Determination of Chlorogenic Acid Based on Carbon Nanotubes Modified Screen-Printed Electrode, 2016.

https://doi.org/10.1016/j.heliyon.2019.e01457